Protein Science (1996), 5:2494–2505. Cambridge University Press. Printed in the USA.

NMR assignments and relaxation studies of *Thiobacillus versutus* ferrocytochrome *c*-550 indicate the presence of a highly mobile 13-residues long C-terminal tail

MARCELLUS UBBINK,[1,4] MARK PFUHL,[2,5] JOHN VAN DER OOST,[3,6] AXEL BERG,[1] AND GERARD W. CANTERS[1]

[1] Leiden Institute of Chemistry, Gorlaeus Laboratories, Einsteinweg 55, 2300 RA Leiden, The Netherlands
[2] European Molecular Biology Laboratory, Meyerhofstrasse 1, D-6900 Heidelberg, Germany
[3] Department of Molecular and Cellular Biology, BioCentrum Amsterdam, Vrije Universiteit, De Boelelaan 1087, 1081 HV Amsterdam, The Netherlands

(RECEIVED July 10, 1996; ACCEPTED September 9, 1996)

Abstract

Cytochrome *c*-550 of *Thiobacillus versutus* functions as an electron transfer protein in a chain of redox proteins that enables *T. versutus* to grow on methylamine. It is a single-heme protein of 134 residues, related to mitochondrial cytochrome *c*. Cytochrome *c*-550, as well as several other bacterial c_2-type cytochromes, contain a C-terminal extension of 13–16 amino acids of unknown function, compared to mitochondrial cytochrome *c*.

NMR experiments were performed to obtain structural and dynamic information on the protein in solution. For this purpose, *T. versutus* cytochrome *c*-550 was labeled with ^{15}N and ^{13}C using ^{13}C-methanol grown *Paracoccus denitrificans* as a host for heterologous expression. NMR assignments were obtained for the ^{1}H, ^{15}N, and ^{13}C nuclei in the backbone and the β-positions of the protein and the secondary structure was determined. ^{15}N-relaxation studies were performed to characterize the dynamic properties of the protein. The results indicate that the main part of *T. versutus* ferrocytochrome *c*-550 exists in solution as a rigid, well-ordered molecule with a secondary structure that is very similar to that of *P. denitrificans* cytochrome *c*-550, as observed in crystals. The C-terminal extension, however, is unstructured and highly mobile. The possible origin and function of the extension are discussed.

Keywords: cytochrome c_2; cytochrome *c*-550; mobility; NMR; *Paracoccus denitrificans*; relaxation; *Thiobacillus versutus*

Cytochrome *c*-550 (or c_2) from *Thiobacillus versutus* is a type I cytochrome *c* (Pettigrew & Moore, 1987), related to mitochondrial cytochrome *c* (Lommen et al., 1990). It functions as an electron carrier in a chain of redox proteins that enables *T. versutus* to utilize methylamine as a carbon and energy source (Van Wielink et al., 1989). Probably, cytochrome *c*-550 is also involved in a mitochondrion-like respiratory chain, as has been demonstrated for *Paracoccus denitrificans* cytochrome *c*-550 (Van Spanning et al., 1995). The gene for *T. versutus* cytochrome *c*-550 has been cloned and expressed in *Escherichia coli* (Ubbink et al., 1992), and several site-specific mutants have been produced to study structural (Ubbink et al., 1994a, 1994c) and functional aspects (Ubbink & Canters, 1993; Ubbink et al., 1994b) of the protein. The methionine at position 100 has been identified as the sixth ligand of the heme. Replacement with a lysine residue resulted in a protein with stable Lys-His coordination of the heme (Ubbink et al., 1994a). No other structural information of cytochrome *c*-550 exists, but the gene sequence indicates that the protein is homologous to cytochrome *c*-550 from *P. denitrificans*, of which the three-dimensional structure has been elucidated by X-ray diffraction (Timkovich & Dickerson, 1976; Benning et al., 1994). The sequences of cytochromes *c*-550 from *T. versutus*, *P. denitrificans* (Van Spanning et al., 1990), and *Thiosphaera pantotropha* (Samyn et al., 1994), as well as the sequence of isocytochrome c_2 from *Rhodobacter sphaeroides* (Rott et al., 1993) indicate the presence of a nonconserved C-terminal

Reprint requests to: G.W. Canters, Leiden Institute of Chemistry, Gorlaeus Laboratories, Einsteinweg 55, P.O. Box 9502, 2300 RA Leiden, The Netherlands.

[4] Present address: University of Cambridge, Department of Biochemistry, Tennis Court Road, Cambridge CB2 1QW, England.

[5] Present address: Department of Biochemistry and Molecular Biology, University College London, Gower Street, London, WC1E 6BT, England.

[6] Present address: Wageningen Agricultural University, Department of Microbiology, H. van Suchtelenweg 4, 6703 CT Wageningen, The Netherlands.

Abbreviations: CSI, chemical-shift index; HSQC, heteronuclear single quantum coherence; NOESY, NOE spectroscopy; TOCSY, total correlation spectroscopy; TOWNY, TOCSY without NOESY; TSP, 3-(trimethylsilyl)-propionate.

extension of 13–16 amino acids in these cytochromes compared to eukaryotic cytochrome *c* (Fig. 1). Electrospray mass spectrometry studies on *T. versutus* cytochrome *c*-550 have shown that this extension is prone to proteolysis; forms of the protein that are up to 13 amino acids shorter have been observed (J. Van Beeumen, pers. comm.). Further degradation is not observed, however, indicating that the main part of the protein is protease resistant. In the crystal structure of *P. denitrificans* cytochrome *c*-550, the C-terminal extension is not observed. Benning et al. (1994) suggest that this is due to proteolytic cleavage.

In order to be able to evaluate the structural effects of site-specific mutations in detail, it was decided to determine the three-dimensional solution structure of *T. versutus* cytochrome *c*-550 using NMR. Here, the ^{1}H, ^{15}N, and ^{13}C NMR resonance assignments of the nuclei in the backbone and the β-positions of *T. versutus* cytochrome *c*-550, as well as the secondary structure of the protein in solution are reported. Also, the relaxation parameters of the ^{15}N-nuclei have been measured to obtain information about the dynamics of the protein, in particular the C-terminal extension. From these data, it is concluded that the main part of cytochrome *c*-550 from *T. versutus* has a secondary structure in solution that is very similar to the one observed for *P. denitrificans* cytochrome *c*-550 in the crystal. The main part is highly ordered, with only a slightly increased mobility in long loops. The C-terminal extension is, however, unstructured and highly mobile.

Results

Labeling of cytochrome c-550

The gene for cytochrome *c*-550 of *T. versutus* has been expressed successfully in *E. coli* (Ubbink et al., 1992). However, the yield of this expression system (1–2 mg/L rich culture medium) is too low to make labeling with ^{13}C feasible, and significant improvement of the yield in this system is not to be expected in view of the difficulties of expression of *c*-type cytochromes in *E. coli* (Ubbink et al., 1992 and references therein). Therefore, a strain of *P. denitrificans* (Pd2131) in which the endogenous gene for cytochrome *c*-550 had been deleted (Van Spanning et al., 1991) was used as host for expression. The gene encoding cytochrome *c*-550 of *T. versutus* and its putative promoter region were introduced in the host on a stable, multicopy plasmid (pEG400) (Gerhus et al., 1990). With this strain, a yield was obtained of 10 mg of cytochrome *c*-550 per liter, when cultured on rich medium. For heteronuclear labeling, a minimal medium was used containing ^{13}C-methanol and ^{15}N-ammonium chloride as carbon and nitrogen source, respectively. Although the yield on minimal medium with methanol is not as high as on other carbon sources (e.g., succinate), ^{13}C-methanol is much less expensive per mole of carbon, making it the compound of choice. Culturing of 12 L with 50 mM ^{13}C-methanol yielded 20 mg of protein (after purification), resulting in a 2.5 mM NMR sample.

In an electrospray mass spectrum (not shown), the sample showed a single peak of 15,540 Da, which indicated that the protein was labeled with ^{13}C and ^{15}N and was of full length (134 amino acids; expected weight 15,542). In between the NMR experiments, the sample was monitored regularly for C-terminal proteolysis. Over a period of months, new peaks appeared in the ^{15}N-HSQC spectra and peaks of residues in the C-terminal extension decreased in intensity (compare Fig. 2A and B; new peaks are indicated by arrows). After about 14 months, a mass spectrum indicated considerable degradation of the C-terminal extension, with multiple protein forms that were shortened up to 11 amino acids (from N134 up to G123). This suggests that all or most peptide bonds in the C-terminal extension are prone to cleavage rather than proteolysis occurring at a single site.

Assignment procedure

To obtain the assignments of the backbone nuclei, first a list of sequential connections was produced based on the HNCA spectrum. This spectrum showed 122 $^{13}C_i^{\alpha}$-$^{15}N_i$-H_i peaks and 118 $^{13}C_{i-1}^{\alpha}$-$^{15}N_i$-H_i peaks out of the maximum of 127 (134 residues minus 7 prolines). Then, spin system identifications were made with the ^{15}N-TOWNY-HSQC spectrum. The coherence transfer from the amide proton into the side chain proved to be poor for a number of residues, as was expected given the considerable helical content of type I cytochromes *c*. Still, enough spin systems could be found to identify amino acid stretches in the HNCA-based list that matched the amino acid sequence of the protein. Remaining ambiguities were solved using NOE crosspeaks ($NH_i - NH_{i+1}$ and $H^{\alpha}/H^{\beta}_{i-1} - NH_i$) in the ^{15}N-HSQC-NOESY spectrum. The backbone assignments were confirmed using the connectivity information supplied by the HNCO/HN(CA)CO pair of spectra. Assignments for the $^{13}C^{\beta}$ nuclei and H^{β} protons, as well as the proline H^{α} protons, were obtained from the ^{15}N-TOWNY-HSQC, ^{15}N-HSQC-NOESY, ^{13}C-HSQC-TOWNY, and ^{13}C-HSQC-NOESY spectra. The results are presented in Table 1.

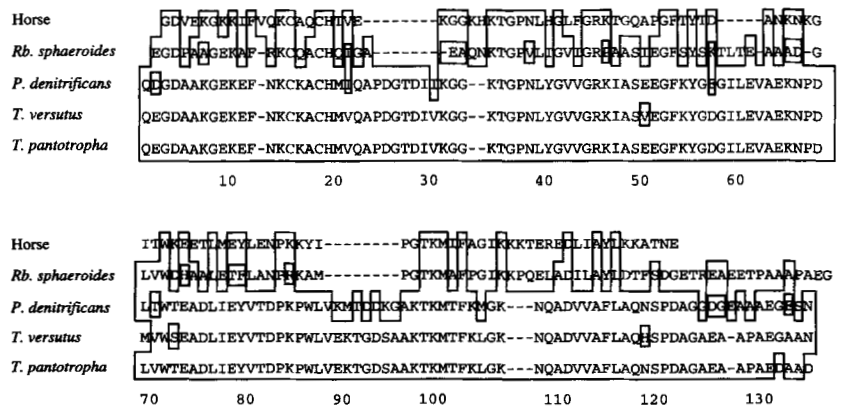

Fig. 1. Alignment of *c*-type cytochromes. Alignment of the amino acid sequences of horse cytochrome *c* (Margoliash et al., 1961), *Rb. sphaeroides* isocytochrome c_2 (Rott et al., 1993), and cytochromes *c*-550 from *P. denitrificans* (Van Spanning et al., 1990), *T. versutus* (Ubbink et al., 1992), and *T. pantotropha* (Samyn et al., 1994). Identical residues are boxed. The numbers refer to the residues in *T. versutus* cytochrome *c*-550.

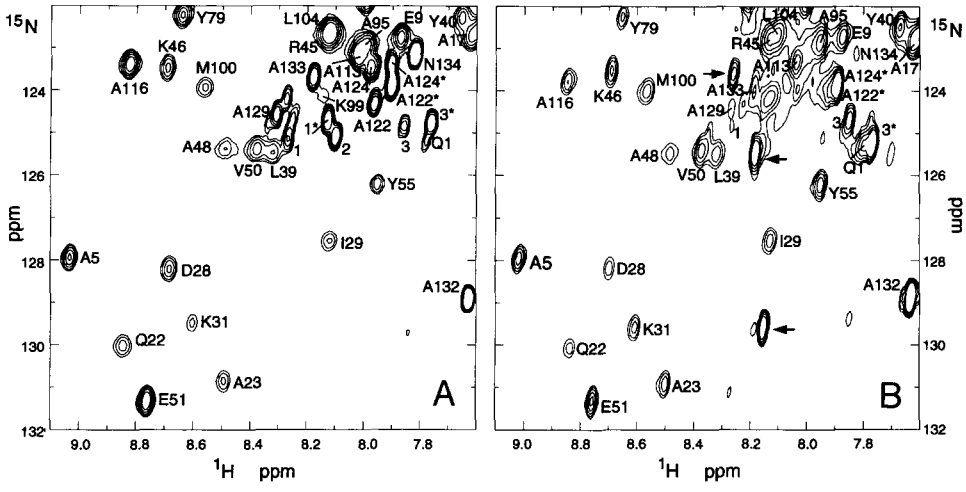

Fig. 2. ^{15}N-HSQC spectra of *T. versutus* cytochrome *c*-550. Parts of ^{15}N-HSQC spectra illustrating the proteolysis of the C-terminal extension. **A:** Fresh sample. **B:** The same sample after 12 months. New peaks are indicated by arrows. Also note the high intensity of peaks of residues in the C-terminal extension (Ala 122–Asn 134). Peaks 1, 1*, and 2 probably represent Ala 126/Ala 127. Peaks 3 and 3* may represent Glu 125. The asterisk indicates double peaks (see text).

Due to the absence of NOE crosspeaks for spin systems in the C-terminal extension, sequential assignments in this part of the protein had to be based solely on the connectivity information from HNCA and HNCO/HN(CA)CO spectra. The 13-amino acid–long stretch contains 7 alanine residues, all of which showed very similar chemical shifts. For this reason, residues Ala 126 and Ala 127 could not be assigned. Assignment of residues Glu 125 and Pro 128 was also ambiguous and therefore no assignments are included in Table 1 for these residues. Some residues in the C-terminal extension of the intact sample appeared to show two peaks in the ^{15}N-HSQC spectrum (Fig. 2) that differed slightly in the ^{15}N and ^{1}H chemical shifts but had connectivities to almost identical ^{13}C resonances and ^{1}H spin systems. This suggests that each peak pair represents a single amino acid residue. For this reason, the ^{15}N and ^{1}H chemical shifts of both peaks are included in Table 1 for each of these residues. A possible explanation for this phenomenon involves *cis–trans* isomerization of Pro 128. Proline isomerization is a slow process on the NMR timescale, and the equilibrium constant is close to 1 in unstructured polypeptides (Schmid et al., 1993). Because Pro 128 is in the middle of the C-terminal extension, which is unstructured and flexible (see below), its isomerization could explain the occurrence of double peaks in the ^{15}N-HSQC spectrum for the residues in the vicinity of Pro 128.

In preparations of *T. versutus* cytochrome *c*-550, residue Gln 1 is usually converted into a pyroglutamate (Ubbink et al., 1992). The ^{1}H and ^{15}N-nuclei of its amide are observed in the NMR spectra (Table 1).

Secondary structure

The secondary structure of *T. versutus* cytochrome *c*-550 in solution was determined on the basis of NOE contacts and the chemical shifts of H^{α}, $^{13}C^{\alpha}$, $^{13}C'$, and $^{13}C^{\beta}$ nuclei using the chemical-shift index (Wishart & Sykes, 1994). The results are presented in Figure 3. Both the CSI and the NOE contact pattern indicate that cytochrome *c*-550 contains five α-helices (helices I, residues 5–15; II, 57–65; III, 73–81; IV, 85–90; and V, 107–117) and the two methods are in reasonable agreement about the number of residues in helices I, III, IV, and V. The N-terminus of helix II is located at residue 57 according to the NOE contact pattern. However, the CSI indicates a smaller helix, starting at residue 60. No H_i^{α}-NH_{i+3} or H_i^{α}-H_{i+3}^{β} NOE contact was observed for Gly 58. This could imply that, at residue 58, the helix is irregular due to the presence of the glycine, causing the difference between the two methods for secondary structure determination. A small β-sheet is formed by two β-strands (residues 19–22 and 27–32). The CSI gives no evidence for the second strand, but strong H_i^{α}-NH_{i+1} and weak H_i^{α}-NH_i NOE contacts suggest an extended structure for these residues. Furthermore, NOE contacts between backbone protons of both strands were observed. According to the CSI, two other, short β-strands are present (residues 97–99 and 102–104). NOE contacts indicate that these residues do form extended structures, but no indications for a β-sheet in this region were found.

In Figure 4, the chemical shifts of the H^{α}, $^{13}C^{\alpha}$, NH, and ^{15}N nuclei are shown for all residues after correction with the "average" values described by Wishart, Sykes, and Richards (Wishart et al., 1991; Wishart & Sykes, 1994), i.e., averages for each amino acid type over a large set of protein chemical shift data. The traces illustrate that all these four nuclei in all assigned residues (except Ala 132) in the C-terminal extension demonstrate chemical shifts that are very close to the average values. This is an indication that the C-terminal extension lacks a well-defined structure, because this would result in a larger spread in the chemical shift values. This is clear in the main part of the protein, where the deviations from the average are much larger, both within and outside secondary structure elements.

Mobility

In the ^{15}N-HSQC spectrum of *T. versutus* cytochrome *c*-550, the residues in the C-terminal extension gave rise to strong peaks (Fig. 2). These residues showed excellent coherence transfer in the ^{15}N-TOWNY-HSQC spectrum, whereas in the ^{15}N-HSQC-NOESY spectrum, essentially no crosspeaks were observed. This is illustrated in Figure 5, in which the slices are shown from both spectra

Table 1. *NMR assignments of T. versutus ferrocytochrome c-550*[a]

Residue	NH	^{15}N	H^{α}	$^{13}C^{\alpha}$	$^{13}C'$	H^{β}		$^{13}C^{\beta}$
Q1	7.79	125.3	4.32	59.4	176.9	2.46	2.02	28.0
E2	8.46	120.7	4.32	56.1	172.3	2.05	1.89	30.3
G3	8.41	108.9	3.90, 3.49	44.2	171.3			
D4	9.67	123.6	4.80	52.3	175.7	2.81	2.50	42.7
A5	9.04	127.9	4.03	55.4	178.4	1.38		17.5
A6	8.22	121.6	4.30	55.0	180.8	1.51		18.0
K7	7.69	120.6	4.04	59.0	179.8	1.90	1.80	32.5
G8	8.91	108.0	4.09, 3.34	46.6	173.5			
E9	7.87	122.8	2.18	58.9	177.3	1.89	1.83	29.2
K10	6.82	116.6	4.03	58.2	180.5	1.97	1.70	32.0
E11	8.12	120.7	4.21	58.2	177.4	2.10	2.05	29.5
F12	8.29	118.3	4.26	60.0	175.4	2.94	2.84	38.2
N13	7.65	117.5	4.31	56.5	176.9	2.98	2.85	38.2
K14	8.29	118.0	4.22	59.0	176.3	2.25	2.18	33.2
C15	7.35	115.9	4.87	54.2	177.5	1.63	0.57	33.9
K16	7.32	117.2	4.66	56.9	175.3	1.55	1.49	32.3
A17	7.60	122.6	3.98	54.7	177.6	1.51		18.8
C18	6.76	110.3	4.15	53.8	170.4	1.59	0.68	39.0
H19	6.59	114.8	3.21	53.4	171.3	0.95	0.59	31.5
M20	6.91	114.2	4.30	51.8	173.0	2.01	1.53	35.8
V21	8.19	116.5	3.98	62.3	172.7	1.54		32.7
Q22	8.85	130.0	4.85	54.5	172.9	1.63	1.63	33.5
A23	8.50	130.9	2.64	50.6	176.0	1.11		18.0
P24				65.0	175.9			
D25	7.35	113.8	4.35	52.9	176.0	2.92	2.47	39.4
G26	8.09	108.0	4.17, 3.16	44.2	173.5			
T27	7.66	116.9	3.74	64.3	173.5	3.87		68.3
D28	8.69	128.2	4.54	55.2	174.5	2.44	2.00	40.8
I29	8.13	127.6	3.84	63.0	176.8	1.46		36.8
V30	7.99	116.0	4.01	62.2	174.9	1.59		35.0
K31	8.61	129.5	4.18	56.5	175.2	1.63	1.52	32.2
G32	7.34	110.7	4.11, 3.93	44.7				
G33	6.92	104.0	3.88, 3.14	43.8	170.5			
K34	7.72	111.9	4.15	55.1	175.8	1.85	1.49	33.4
T35	7.30	117.9	3.96	65.8	173.2	3.99		69.7
G36	7.43	104.6	3.66, −0.62	40.7				
P37			3.50	60.4	174.8	1.16	1.09	31.7
N38	7.94	119.2	3.88	52.9	176.0	2.73	2.68	37.5
L39	8.33	125.5	3.89	53.6	176.2	1.22	0.80	41.9
Y40	7.66	122.3	3.73	60.0	176.5	2.54	2.54	38.8
G41	7.99	117.2	3.70, 3.70	46.3	173.8			
V42	7.03	116.6	3.64	63.6	174.1	1.66		31.7
V43	7.72	119.8	3.58	65.3	175.8	1.94		29.7
G44	8.93	116.1	4.35, 3.43	44.5	172.5			
R45	8.13	122.7	4.64	55.0	175.4	2.19	2.19	32.9
K46	8.70	123.5	4.45	57.4	177.4	1.85	1.71	32.2
I47	7.16	125.2	3.37	61.4	173.6	1.71		36.2
A48	8.50	125.4	3.48	52.5	175.4	0.71		17.7
S49	8.21	108.1	4.78	58.0	174.9	4.17	3.30	65.5
V50	8.38	125.4	3.89	64.8	176.4	2.31		30.6
E51	8.77	131.4	4.16	58.0	177.2	2.07	2.02	29.5
G52	8.89	113.0	4.17, 3.69	45.3	172.8			
F53	7.48	121.2	4.16	58.5	174.0	2.66	2.27	39.6
K54	7.09	128.6	4.41	54.2	173.6	1.59	1.39	29.9
Y55	7.96	126.2	5.04	59.6	177.0	3.67	2.85	40.7
G56	11.35	109.7	4.33, 4.33	44.5	172.8			
D57	8.12	115.2	4.40	56.7	179.8	2.79	2.68	40.4
G58	7.94	108.9	4.07, 3.92	47.9	174.0			
I59	9.91	124.6	4.20	65.0	177.3	1.66		30.5
L60	7.61	122.8	4.10	57.6	179.3	1.96	1.51	41.1

(*continued*)

Table 1. *Continued*

Residue	NH	^{15}N	H^{α}	$^{13}C^{\alpha}$	$^{13}C'$	H^{β}		$^{13}C^{\beta}$
E61	8.00	121.9	4.11	58.7	178.1	2.52	2.30	28.0
V62	7.60	119.6	2.98	67.4	177.5	2.54		30.8
A63	7.28	121.2	3.87	54.3	178.5	1.37		18.5
E64	8.16	117.7	3.89	58.6	178.2	2.14	2.06	29.6
K65	7.90	115.0	4.12	57.0	175.6	1.94	1.74	33.3
N66	7.51	115.9	5.13	50.6	171.6	2.85	2.36	40.7
P67			4.53	64.9	176.1	2.30	1.93	31.8
D68	8.33	115.2	4.65	53.6	175.4	2.74	2.56	41.0
M69	7.48	121.4	4.16	57.4	175.2	1.92	1.87	34.4
V70	8.04	119.1	4.77	57.7	175.3	1.58		35.1
W71	8.50	120.4	4.72	58.0	176.7	3.97	2.96	30.3
S72	8.20	120.8	4.94	56.1	174.3	4.38	4.16	66.2
E73	9.59	121.5	3.91	61.6	176.9	2.07	2.07	28.8
A74	8.50	118.8	4.06	55.5	180.4	1.42		18.6
D75	7.86	116.9	4.81	57.8	177.4	3.13	3.13	41.8
L76	8.57	120.7	3.75	58.1	177.8	2.21	1.16	43.6
I77	8.16	117.7	3.24	66.1	177.4	1.89		38.3
E78	7.52	119.9	3.89	59.6	177.9	2.29	2.29	30.0
Y79	8.65	122.2	3.31	61.7	175.1	2.23	1.61	38.5
V80	7.99	110.0	2.31	63.5	174.9	1.74		31.3
T81	6.81	115.4	4.27	65.3	173.9	4.18		68.6
D82	6.12	110.0	4.03	53.1	172.9	2.60	2.50	40.1
P83			3.42	66.0	177.1	1.02	0.96	33.0
K84	8.19	114.4	3.88	61.9	174.2	1.77	1.62	29.6
P85			4.08	65.4	178.0	2.13	1.73	30.4
W86	7.00	119.5	4.08	62.7	176.7	3.72	3.09	29.1
L87	8.31	117.5	3.60	58.0	180.7	2.12	0.96	42.7
V88	8.21	120.2	3.29	65.9	178.1	1.91		29.8
E89	8.02	121.2	3.83	58.9	178.2	2.06	1.96	28.9
K90	7.54	113.2	3.96	55.4	177.1	1.25	1.15	33.0
T91	7.46	105.2	4.19	62.0	175.4	3.89		71.5
G92	8.29	111.8	4.01, 3.71	45.8	172.6	1.77	1.69	35.4
D93	8.15	119.4	4.73	51.5	175.3	3.19	2.44	39.9
S94	8.62	119.7	4.02	60.7	173.6	3.83	3.83	62.7
A95	8.00	123.0	4.31	51.0	176.3	1.34		19.1
A96	7.11	122.8	3.94	53.4	176.1	1.16		18.9
K97	8.17	119.8	4.56	54.6	176.1	1.77	1.69	35.4
T98	8.15	114.5	4.42	59.6	172.7	3.67		69.5
K99	8.15	124.1	4.59	56.1	175.3	1.87		
M100	8.57	123.9	3.33	54.7	172.4	−0.01	−2.56	29.3
T101	7.75	119.5	3.79	60.4	172.3	4.40		66.9
F102	5.91	120.8	4.08	57.6	169.8	2.99	1.19	42.6
K103	5.82	119.8	3.55	54.1	171.8	1.30	1.13	34.6
L104	8.14	122.7	4.31	53.2	173.7	1.65	1.09	45.0
G105	8.26	110.6	4.18, 3.50	45.3	172.8			
K106	7.09	116.1	4.49	54.9	174.1	1.73	1.59	36.0
N107	8.82	111.7	4.56	55.0	175.7	3.23	3.07	36.7
Q108	10.10	119.9	3.76	60.5	178.0	1.82	1.82	29.0
A109	8.92	117.6	3.85	54.7	179.7	1.31		17.5
D110	7.32	117.2	4.20	57.3	177.3	2.80	2.64	40.1
V111	7.73	119.8	3.91	66.7	176.8	1.54		22.2
V112	8.12	120.7	3.62	67.7	175.6	2.05		31.2
A113	8.02	123.1	4.17	55.0	180.3	1.37		17.6
F114	7.82	118.8	4.24	60.9	175.9	3.54	3.30	38.0
L115	8.04	119.1	3.55	57.0	180.1	1.99	1.09	40.8
A116	8.83	123.4	3.70	54.6	178.4	1.41		18.0
Q117	7.28	116.8	3.82	57.2	175.3	2.35	1.70	28.3
H118	6.67	115.7	4.51	54.0	171.2	2.84	2.37	28.0
S119	6.89	112.7	4.45	55.0	171.3	3.79	3.69	64.4
P120			4.28	63.4	176.3	2.25	1.90	32.1

(*continued*)

Table 1. *Continued*

Residue	NH	^{15}N	H^{α}	$^{13}C^{\alpha}$	$^{13}C'$	H^{β}		$^{13}C^{\beta}$
D121	8.44	119.2	4.57	54.2	175.5	2.73	2.55	40.7
A122	7.97	124.3	4.22	52.9	177.8	1.37		
A122*	7.91	123.9	4.21	52.9		1.39		
G123	8.31	107.7	3.92, 3.92	45.2	172.4			
G123*	8.26	108.1	3.85, 3.85	45.2				
A124	7.98		123.5	52.0		1.36		
A124*	7.91	123.4		52.3		1.36		
E125								
A126								
A127								
P128				62.7				
A129	8.32	124.6	4.26	52.3	176.0	1.35		
E130	8.32	120.0		56.5		2.03	1.88	
E130*	8.28	119.8	4.22	56.1		2.03	1.88	
G131	8.30	110.1	3.89, 3.89	45.1				
A132	7.63	128.9	4.11	53.6		1.30		
A133	8.19	123.7	4.28	52.1	175.9	1.35		
N134	7.83	123.2	4.39	54.5	178.8	2.73	2.59	

[a]Proton assignments, ±0.02 ppm; other nuclei ±0.1 ppm. Conditions: 2.5 mM protein in water/D_2O (90:10) pH 6.0, at 310 K. Double peaks (see text) are indicated with an asterisk.

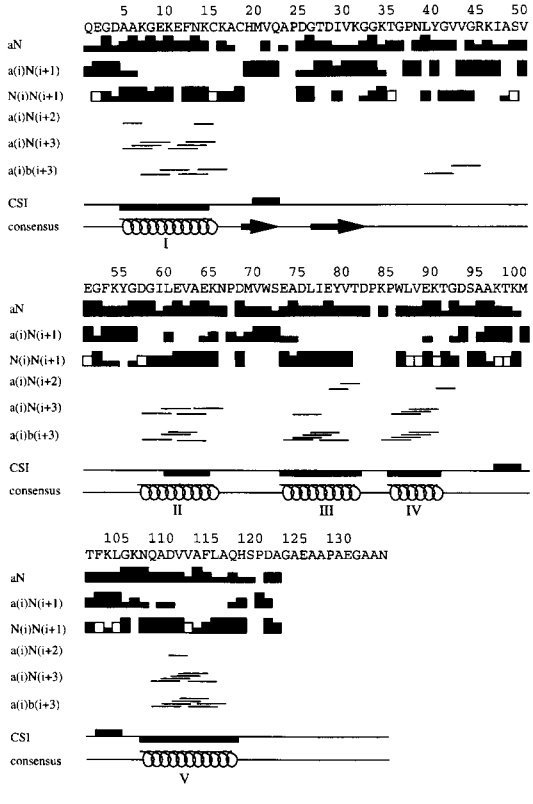

Fig. 3. Secondary structure of *T. versutus* cytochrome *c*-550. Short- and intermediate-range backbone NOE contacts are shown for each residue. Bar heights represent the relative intensity of the NOE crosspeak. Open bars indicate that no NOE crosspeak could be observed due to chemical shift overlap of the two protons. a, H^{α}; N, NH; b, H^{β}; *i*, any residue number. The CSI is positive (bar above line) for β-strands and negative (bar beneath line) for α-helices. In the "consensus" line, a spiral represents an α-helix (I–V) and an arrow represents a β-strand.

for Glu 73 and Glu 130, residues in the main part of the protein and in the C-terminal extension, respectively. These observations suggested that the residues in the C-terminal extension have high transverse relaxation times, indicative of high local mobility. The

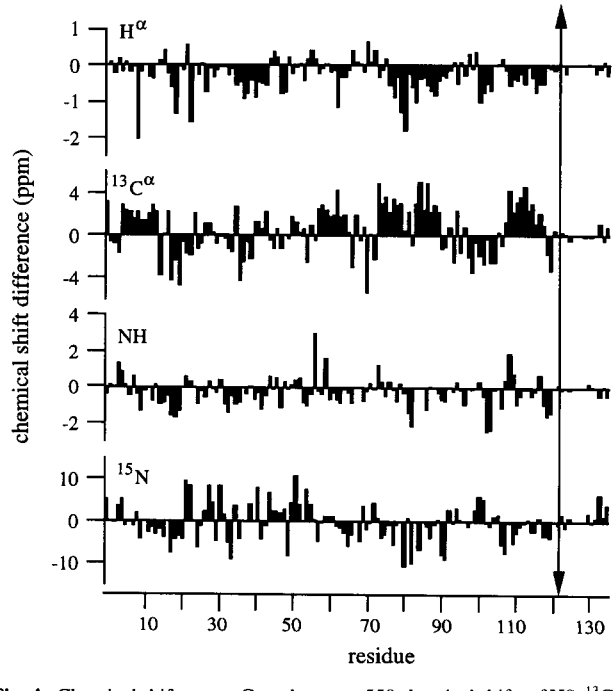

Fig. 4. Chemical shift traces. Cytochrome *c*-550 chemical shifts of H^{α}, $^{13}C^{\alpha}$, NH, and ^{15}N nuclei have been plotted for all residues after subtraction of "average" values as defined in Wishart et al. (1991) and Wishart and Sykes (1994). The double-sided arrow indicates the separation between the main part of the protein (left of arrow) and the C-terminal extension (right of arrow).

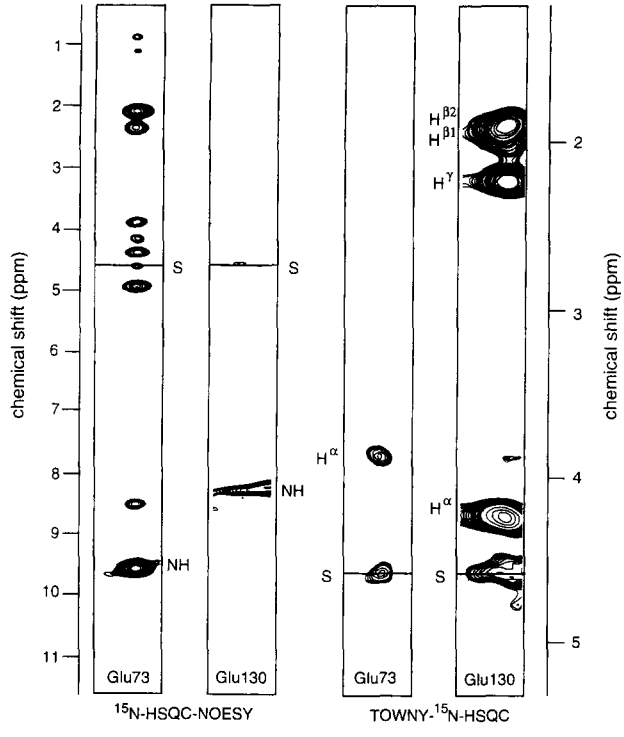

Fig. 5. Mobility in the C-terminal extension. Strips from the ^{15}N-HSQC-NOESY and ^{15}N-TOWNY-HSQC spectra are displayed, showing the NOE and TOCSY crosspeaks, respectively, from the amide protons of residues E73 (main part of the protein) and E130 (C-terminal extension). NH, diagonal peaks; S, chemical shift position of solvent; H^{α}, $H^{\beta 1}$, $H^{\beta 2}$, and H^{γ}, chemical shift positions of the glutamate protons.

absence of NOE crosspeaks supports the finding that this part of the protein lacks structure.

To corroborate these findings, ^{15}N-relaxation measurements were performed. Relaxation parameters were extracted for all 103 assigned residues that gave sufficiently resolved peaks in the ^{15}N-HSQC spectrum. The relaxation parameters T_1, T_2, and heteronuclear NOE are shown in Figure 6A, B, and C, respectively. For most residues, the values are rather uniform (average values $T_1 = 657 \pm 58$ ms, $T_2 = 98 \pm 15$ ms, and NOE $= 0.79 \pm 0.12$), with the only small deviations for residues Asp 25–Val 30, Lys 54–Asp 57, and Asp 93–Ala 95. Major deviations, however, are observed for residues in the N-terminus (Gln 1 and Glu 2) and the C-terminal extension (Ala 122–Asn 134). The termini are mainly characterized by the strong negative heteronuclear NOE values, indicative of fast internal motion. Consistent with that, the values of T_1 and T_2 are much longer than the average values. The relaxation parameters were analyzed (Fig. 6) by the Lipari–Szabo approach in the extended form (Clore et al., 1990) using the following spectral density function $J(\omega)$:

$$J(\omega) = \frac{2}{5}\left[\frac{S^2\tau_R}{1+(\omega\tau_R)^2} + \frac{(1-S_f^2)\tau_e'}{1+(\omega\tau_e')^2} + \frac{(S_f^2-S^2)\tau_i'}{1+(\omega\tau_i')^2}\right] \quad (1)$$

where $\tau_e' = \tau_e\tau_R/(\tau_e + \tau_R)$, $\tau_i' = \tau_i\tau_R/(\tau_i + \tau_R)$, τ_e and τ_i are the effective correlation times for internal motions on a fast (<200 ps) and intermediate (ns) time scales, respectively, $S^2 = S_f^2S_s^2$ is the square of the generalized order parameter characterizing the amplitude of the internal motions, and S_f^2 and S_s^2 are the squares of the order parameters of the fast and slow internal motions, respectively. The overall tumbling time, τ_R, was calculated from the T_1/T_2 ratios of the residues with T_1 and T_2 values within one standard deviation of the average value, and is 6.6 ± 0.4 ns. The majority of residues (61 residues, 59%) could be fitted with Equation 1 assuming only very fast internal motions, faster than 25 ps (thermal vibrations), indicative of a rather rigid structure. In this case, $S_s^2 = 1$ and $\tau_e \rightarrow 0$, implying that the second and the third term in Equation 1 approach zero (models 1 and 2). Only 16 residues (16%) showed a strong contribution from internal motions with local correlation times bigger than 25 ps ($S_s^2 = 1$, $\tau_e > 25$ ps, models 3 and 4). Most of these residues are located in the termini, with values for the local correlation time τ_e between 50 and 250 ps in the C-terminal extension and around 100 ps at the N-terminus (Fig. 6E). All other residues that were fitted with a model containing τ_e, had values around 25 ps. Motions on an intermediate time scale of up to a few ns (correlation time τ_i) were found for only six residues (6%), which were fitted assuming that $S_s^2 < 1$ and $\tau_e \rightarrow 0$ (model 5). Four of these are found near the beginning of the C-terminal extension (residues 118 and 121–123), one in the long loop connecting helices I and II (39), and one at the N-terminus (3). The S_f^2 and τ_i values are shown in Figure 6F and G, respectively. Contributions from chemical exchange on the time scale of milliseconds–seconds were found in 25 residues (24%, fitted with models 2 and 4 and shown in Fig. 6H). Again, most of these were found at the C-terminal extension, at the N-terminus and in the loops connecting helices I and II and IV and V. The parameters and the numbers of residues fitted with each model are shown in Table 2.

In conclusion, the main part of cytochrome *c*-550 exists in solution as a rigid structure ($S^2 \sim 0.8$) with slightly more dynamic loops in the regions of Met 20–Val 30 and Thr 91–Leu 104. In these regions, somewhat increased T_1 values are opposed by slightly decreased T_2 values. As shown by the values of R_{ex} in Figure 6H, this is indicative of exchange processes in these regions. In the Thr 91–Leu 104 region, fast internal motions on the picosecond time scale also contribute to the relaxation. Consistent with the increased mobility in these two regions, the order parameters are reduced, although only very little, to $S^2 \sim 0.7$. The first 3 residues of the protein and the 13 residues in the C-terminal extension demonstrate a high mobility. Because all the relaxation parameters are in agreement with this conclusion (long T_1 and T_2 relaxation times and heteronuclear NOE values that are close to zero or even negative), the Lipari–Szabo analysis yields very low order parameters ranging from $S^2 \sim 0.5$ down to $S^2 \sim 0.03$ for these residues (Figure 6D).

Table 2. *Models used in relaxation analysis*

Model	Parameters	Residues fitted
1	S^2	61
2	S^2, R_{ex}	20
3	S^2, τ_e	11
4	S^2, τ_e, R_{ex}	5
5	S^2, S_f^2, τ_i	6

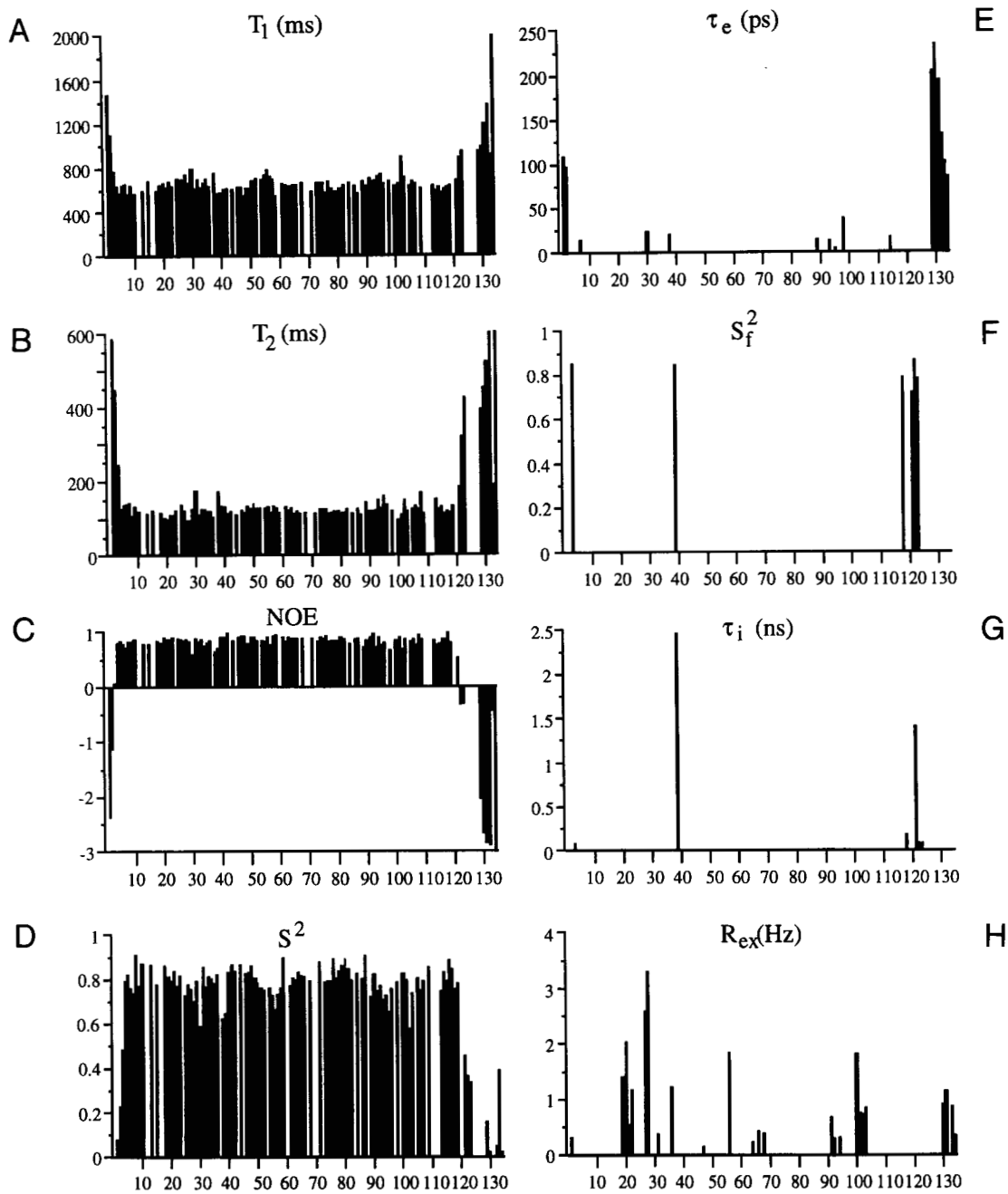

Fig. 6. Relaxation of backbone ^{15}N-nuclei. ^{15}N relaxation parameters as measured (T_1, T_2, NOE) and obtained from a model-free analysis (S^2, S_f^2, τ_e, τ_i, R_{ex}). The T_2 values of A132 and N134 were truncated at 600 ms. The correct values are 820 ms for A132 and 920 ms for N134.

Discussion

Secondary structure

A comparison between the secondary structures of *T. versutus* cytochrome *c*-550, derived from the NMR data, and *P. denitrificans* cytochrome c-550, as observed in the crystal structure, shows that they are nearly identical (Fig. 7), which is in agreement with the high homology (112 identical residues of 134) in the primary structures (Fig. 1).

It is interesting to note that the CSI predicts the secondary structure rather reliably (as judged by the NOE contact data), because in cytochromes, the ring current effect of the heme has a considerable effect on the chemical shift of nearby protons. In principle, that could flaw the CSI. At least for cytochrome *c*-550, that appears not to be the case. The reason is probably that few backbone atoms are near the heme, which is essentially surrounded by side chains. In the *P. denitrificans* cytochrome *c*-550 crystal structure, only seven residues have backbone or C^β atoms within 5 Å of the pyrrole ring.

The knowledge of the secondary structure was used to compare the ^{15}N chemical shifts of the nuclei within and outside the α-helices of cytochrome *c*-550. Braun, Wider, and Wüthrich (Braun et al.,

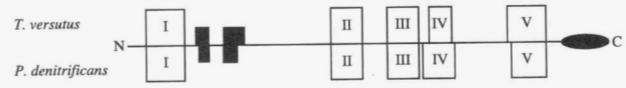

Fig. 7. Secondary structure comparison. Comparison of the secondary structure of *T. versutus* cytochrome *c*-550, based on NMR data (this work), and *P. denitrificans* cytochrome *c*-550, derived from crystallographic data (Benning et al., 1994). Open boxes, α-helices (I–V); solid boxes, β-strands; solid oval, C-terminal extension. N, C, N-, and C-terminus, respectively.

1994) have described a method to calculate "sequence corrected random coil" values for ^{15}N-amide nuclei. The purpose of the method is to obtain a random coil value for each residue in a polypeptide chain that is corrected for the effect of the preceding residue on the chemical shift. These random coil values were compared with those described by Wishart, Sykes, and Richards (Wishart et al., 1991), which are not true random coil values, but averages for each residue over a large set of protein chemical shift data. When applied to the chemical shifts of the 124 assigned ^{15}N-amide nuclei of *T. versutus* cytochrome *c*-550, both correction methods decreased the standard deviation of the set of chemical shifts from 5.8 to 4.2 ppm. Thus, for this data set, the sequence correction method does not result in an additional decrease in the spread of the chemical shifts as compared to the simpler correction using the average chemical shifts. The latter was used in Figure 4, bottom trace. On average, the chemical shifts of the 40 ^{15}N-nuclei in α-helices were shifted upfield by 1.6 and 1.4 ppm, according to the "Braun-values" and the "Wishart values," respectively. As expected (Wishart et al., 1991), this effect of the secondary structure on the chemical shift is small compared to the spread in the data.

Mobility

The relaxation measurements indicate that the main part of cytochrome *c*-550 has a rigid structure, with some mobility in the two long loops connecting helices I and II and helices IV and V. In the crystal structure of *P. denitrificans* cytochrome *c*-550, most residues in these loops make close contacts with the heme and the hydrophobic core. Small parts, however, protrude far into solution (residues 25–30, 51–58, and 91–96). It is exactly these residues that show slightly increased mobility (Fig. 8). A similar behavior of loops has been observed in other proteins, e.g., interleukin-4 (Redfield et al., 1992) or the spectrin repeat (Pascual et al., 1996). The rather compact fold and the presence of the heme as a covalent linker may prevent a higher mobility of the loops. The C-terminal extension (residues 122–134) shows a high mobility compared to the main part of the protein, but the effective correlation times τ_e are rather long and close to the range of the time constant of the intermediate motion (Fig. 6E). Residues 118 and 121–123 show motion on the intermediate time scale (Fig. 6F,G). The mobility therefore appears to increase from an intermediate time scale (nanoseconds) at the start of the C-terminal extension to the picosecond range near the C-terminus (Fig. 8). The mobility of even the last residues is, however, still in upper range of τ_e values, closer to the intermediate time scale motions than to the purely thermal vibrational motions (faster than 25 ps). The transition in time scales may be explained by an increasing distance from the covalent linkage to the rigid core of the protein or a gradual decrease in interactions of C-terminal residues with the rest of the protein. The rather high τ_e values indicate unspecific transient interactions of the C-terminal extension with the rest of the protein. The residues in the C-terminal extension show a relatively uniform chemical exchange with $R_{ex} \sim$ 1 Hz (Fig. 6H). The isomerization of Pro 128 (see Results) could be one of the causes of this exchange.

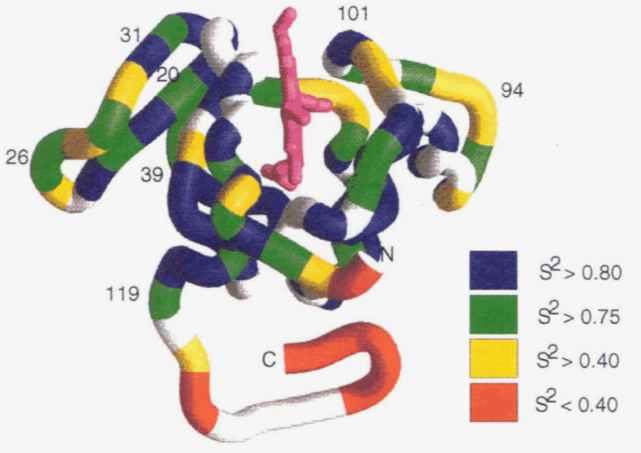

Fig. 8. Order parameters of *T. versutus* cytochrome *c*-550 The backbone of *P. denitrificans* cytochrome *c*-550 (Timkovich & Dickerson, 1976) was colored according to order parameters S^2 (Fig. 6D) of the ^{15}N-nuclei of *T. versutus* cytochrome *c*-550. Residues for which no order parameter could be determined are in white. The heme is shown in sticks representation. N, C, N-, and C-terminus, respectively. Some residue numbers are shown.

C-terminal extension

An alignment of the sequences of bacterial cytochromes c_2 shows variation in the position of the final residue of up to 18 amino acids (not shown). In the crystal structures of *Rhodospirillum rubrum* (Salemme et al., 1973), *Rhodobacter capsulatus* (Benning et al., 1991), and *Rhodobacter spaeroides* (Axelrod et al., 1994) cytochromes c_2, the protein chain ends two to four residues after the C-terminal helix, but in cytochrome c_2 of *Rhodopseudomonas viridis* (Miki et al., 1994), this helix is shorter and the protein contains an extra turn after this helix. A long (13–16 residues) C-terminal extension is a feature observed so far in four c_2 cytochromes. Three of these are very similar, whereas the fourth, isocytochrome c_2 from *R. sphaeroides*, is more distantly related and has a sequence that appears to be an intermediate between the cytochromes *c*-550 and mitochondrial cytochrome *c* (Fig. 1). In this study, it was found that the extension is unstructured, as judged by the chemical shifts of the backbone nuclei and the absence of any NOE cross-peaks for these residues. The good coherence transfer, observed in the TOCSY spectra, and the relaxation measurements have shown that this stretch of amino acids is highly mobile. These findings are in agreement with the observation that the extension is prone to proteolysis.

It might be that the extension is not originally part of the cytochrome protein and may have arisen because of an accidental DNA insertion or stop codon mutation. Alternatively, it cannot be excluded that the common origin of the cytochromes c_2 was a longer protein or part of a complex. The fact that cytochrome *c*-like domains are found in some proteins (Moore & Pettigrew, 1990) could support this idea, although these domains could also have arisen as a consequence of gene fusions. Because the extension is found in a group of cytochromes c_2, one of which is not very homologous to the others, there may be some advantage in its

presence. The C-terminal extension is the part of the protein that is least conserved and this "protein tail" is located on the side of the protein opposite of the heme edge. Hence, it is far removed from the part of the protein surface, which is involved in electron transfer reactions (Ubbink & Canters, 1993; Ubbink et al., 1994b). However, one feature common among the four sequences is that they contain a relatively large number of negative charges. Located at the back of the protein, these will increase the dipole moment of the cytochromes, which can be expected to be favorable given the highly electrostatic nature of the interactions between the cytochromes and their redox partners. At present, experiments are in progress to remove the C-terminal extension by genetic means in order to analyze whether this has any effect on the function of the protein.

Conclusions

This work has shown that the main part of cytochrome *c*-550 exists as a well-ordered, rigid protein in solution, with a clearly defined secondary structure of five α-helices and a small β-sheet. The C-terminal extension of 13 residues is, however, unstructured and mobile. The NMR assignments obtained in these studies form the basis of the determination of the tertiary structure of the protein in solution.

Materials and methods

Sample preparation

The gene for *T. versutus* cytochrome *c*-550 and its putative promoter region (*Sph* I–*Sph* I restriction fragment of pMU8) (Ubbink et al., 1992) were inserted in vector pEG400 (Gerhus et al., 1990) and conjugated from *E. coli* TG1 to *P. denitrificans* Pd2131 via triple conjugation using *E. coli* HB101/pRK2020 (De Gier et al., 1994). In *P. denitrificans* Pd2131, the native gene for cytochrome *c*-550 has been deleted (Van Spanning et al., 1991). Plasmid pEG400 is stable in both hosts. The conjugant was cultured to log phase in rich medium (Brain Heart Infusion broth) at 30 °C and inoculated (1:20) in minimal medium (Chang & Morris, 1962), supplemented with a trace element solution (Van Spanning et al., 1990) and with 100 mM methylamine and 30 mM ammonium chloride as carbon and nitrogen source, respectively. After incubation for 24 h, the culture was used for inoculation (1:20) of minimal medium with 50 mM methanol and 30 mM ammonium chloride (both unlabeled), which was cultured for 65 h and diluted 1:10 to 1 L with minimal medium containing 10 mM ^{13}C-methanol (99.2% in ^{13}C, ISOTEC, Miamisburg, Ohio) and 8 mM ^{15}N-ammonium chloride (99.8%, ISOTEC). After 24 h of incubation, this culture was diluted to 12 L in the same medium and, after another 24 and 48 h, extra ^{13}C-methanol (20 mM twice) was added. After 72 h, the cells were harvested. In this procedure, inoculation volumes are large and the methanol concentration is kept low to ensure that the bacteria adapt successfully and will use methanol as the carbon source.

The cells were concentrated and lysed using a French press in the presence of 0.1 mM phenylmethylsulfonyl fluoride and 40 μg/mL DNase. Cell debris was removed by ultracentrifugation and cytochrome *c*-550 was purified as described (Ubbink et al., 1992). The yield was 20 mg of pure protein. The electrospray mass spectrum of the protein showed a single peak at 15,540 Da, indicating essentially full enrichment in ^{13}C and ^{15}N.

The protein was concentrated and reduced with a tiny amount of dithionite and 0.1 equivalent of sodium ascorbate and 10% D_2O was added. In the NMR tube, the pH was adjusted to 6.0 with small aliquots of NaOH and HCl and the sample was flushed with argon. The cytochrome showed slow re-oxidation and was reduced again about every two months. After reduction, the pH was corrected to 6.0 and the sample was flushed with argon again.

NMR experiments

All measurements were performed on a 2.5-mM ^{15}N-,^{13}C-enriched sample of *T. versutus* ferrocytochrome *c*-550 in water/D_2O (90:10) at pH 6.0 and 310 K. Spectra were recorded on three Bruker NMR spectrometers (AMX500/600 at EMBL, Heidelberg, and DMX600 at Leiden University). Water suppression was accomplished by presaturation in the HNCA, HNCO, and the HN(CA)CO experiments, by WATERGATE in all experiments involving only ^{15}N, and by scrambling gradients implemented in z-filters in the ^{13}C-resolved NOESY and TOWNY experiments. ^{15}N- and ^{13}C-resolved 3D TOWNY experiments were obtained from the original experiments by substituting the NOESY mixing time by the TOWNY mixing scheme. Phase-sensitive spectra in the indirect dimensions were obtained by the States-TPPI method (Marion et al., 1989). Otherwise the experiments were performed as described in the original references (see Table 3), with the following settings. Refocusing delays used in all experiments were: H-N, 2.4 ms; H-C, 1.4 ms; N-C$^{\alpha}$, 11.1 ms; N-CO, 11.5 ms; C$^{\alpha}$-CO, 3.5 ms. Broadband decoupling during acquisition was done with the GARP sequence (Shaka et al., 1985) with a field strength of 1.32 kHz for ^{13}C and 1.28 kHz for ^{15}N. ^{1}H was decoupled in the HN(CA)CO using the DIPSI-2 pulsetrain (Shaka et al., 1988) at a field strength of 6.25 kHz. Off-resonance ^{13}C-pulses in the triple-resonance experiments were performed using the shaped-pulses option in UXNMR, with the shape of a sinc function with 128 steps at a field strength of 2.5 kHz. ^{15}N-relaxation times were determined from eight experiments for T_1 (10, 40, 120, 200, 300, 500, 700, and 900 ms) and T_2 (4, 24, 38.4, 55.2, 84.0, 110.4, 151.2, and 192 ms). The ^{15}N-^{1}H heteronuclear NOE was obtained as the ratio of peak intensities in HSQC experiments with and without proton saturation for 3 s. Further details on the experiments are given in Table 3. 3D spectra were processed with Azara on a 16 processor Silicon graphics power challenge computer. Residual water in the ^{13}C-resolved NOESY spectrum was further suppressed by means of a Karhunen–Loewe transformation as implemented in NMR3D (Mitschang et al., 1991). Prior to zero-filling and window multiplication, indirect dimensions were expanded by linear prediction (Barkhuisen et al., 1985). Usually, no more than half the number of acquired real points were added in this way. Spectra were multiplied subsequently with a gaussian function having a linewidth of 10 Hz and a gaussian factor of 0.1 in the acquisition dimension and with a $\pi/2$ shifted sine window in all indirect dimensions. Baseline correction was performed with a polynomial function. Spectra were analyzed and plotted using AURELIA (Neidig et al., 1995) and ANSIG (Kraulis, 1989; Kraulis et al., 1994) on Silicon graphics INDIGO and INDY workstations. Chemical shifts were referenced to the ^{1}H resonance of TSP according to Wishart et al. (1995). Peak volumes for the T_1, T_2, and heteronuclear NOE were obtained by integration in AURELIA. Volumes were plotted against the time increments and the curves were fitted against simple decaying exponentials in *Mathematica* (Wolfram, 1988). Values of T_1, T_2, and ^{1}H-^{15}N NOE were then fitted by different motional models

Table 3. *Heteronuclear NMR experiments*[a]

Experiment		SW	ptAQ	t_{max} (ms)	ptPR	NS	Ref.
^{15}N-HSQC	F1	42 ppm	256	25.2	512	16	1,2
	F2	4.8 ppm	1k	177.3	2k		
^{13}C-HSQC	F1	80 ppm	512	12.8	1024	32	3
	F2	16 ppm	2k	106.6	2k		
^{15}N-NOESY-HSQC	F1	15 ppm	180	5.0	512	16	2
	F2	42 ppm	80	7.9	256		
	F3	4.8 ppm	512	88.7	512		
^{15}N-TOWNY-HSQC	F1	15 ppm	160	4.4	256	16	2,4
	F2	42 ppm	80	7.9	128		
	F3	4.8 ppm	512	88.7	512		
^{13}C-HSQC-NOESY	F1	78 ppm	136	2.8	256	16	5
	F2	14 ppm	144	4.3	512		
	F3	19 ppm	1k	90.2	1k		
^{13}C-HSQC-TOWNY	F1	78 ppm	136	2.8	256	16	5,4
	F2	14 ppm	144	4.3	512		
	F3	19 ppm	1k	90.2	1k		
HNCA	F1	42 ppm	64	6.2	128	16	6
	F2	35 ppm	64	3.7	128		
	F3	4.8 ppm	256	44.3	512		
HNCO	F1	42 ppm	64	6.2	128	16	6
	F2	25 ppm	44	3.5	128		
	F3	4.8 ppm	256	44.3	512		
HN(CA)CO	F1	42 ppm	64	6.2	128	16	7
	F2	25 ppm	64	3.5	128		
	F3	4.8 ppm	256	44.3	512		
^{15}N-T_1	F1	42 ppm	200	39.4	512	32	8
	F2	4.8 ppm	1k	177.3	2k		
^{15}N-T_2	F1	42 ppm	200	39.4	512	32	8
	F2	4.8 ppm	1k	177.3	2k		
^{15}N-^{1}H-NOE	F1	42 ppm	200	39.4	512	96	9
	F2	4.8 ppm	1k	177.3	2k		

[a] F1, F2, F3, dimensions; SW, spectral width; t_{max}, acquisition time; ptAQ, number of real points acquired; ptPR, number of real points after processing as a result of linear prediction and zero filling; NS, number of scans added for each increment in t_1 or t_2; Ref., reference as follows: 1, Bax et al. (1989); 2, Sklènar et al. (1993); 3, Stonehouse et al. (1994); 4, Kadkhodaei et al. (1993); 5, Majumdar and Zuiderweg (1993); 6, Grzesiek and Bax (1992); 7, Clubb et al. (1992); 8, Kay et al. (1992); 9, Kay et al. (1989).

based on the model-free approach (Lipari & Szabo, 1982a, 1982b) and its recent extension to intermediate time scales (Clore et al., 1990), as well as a correction for exchange effects on T_2. First, average values for T_1 and T_2 were calculated discarding all those deviating more than one standard deviation. From the ratio of T_1/T_2, the overall tumbling time was calculated, which was kept fixed in all subsequent calculations. Five models were used in the fits (Mandel et al., 1995). Fitting was started with the simplest model (model 1, Table 2). If the fitted data resulted in a deviation of more than 4% (the estimated experimental error) from the experimental values, the next model (model 2) was tried. This was repeated with more complicated models until a fit within the experimental error was obtained. However, a more complicated model was chosen over a simpler one only if it was significantly better, i.e., if it decreased the fit error by at least the experimental error.

Supplementary material in Electronic Appendix

The assignments in Table 1 as well as additional assignments of side-chain and heme nuclei are provided in a table format as supplementary material in the Electronic Appendix.

Acknowledgments

We thank Annalisa Pastore for her help with the experiments and for fruitful discussion. Johan Kemmink, Goran Karlsson, and Cees Erkelens are acknowledged for their help with the spectrometers.

References

Axelrod HL, Feher G, Allen JP, Chirino AJ, Day MW, Hsu BT, Rees DC. 1994. Crystallization and X-ray structure determination of cytochrome c_2 from *Rhodobacter sphaeroides* in three crystal forms. *Acta Crystallogr D 50*:596–602.

Barkhuisen H, de Beer R, Bovee WMMJ, van Ormondt D. 1985. Retrieval of frequencies, amplitudes, damping factors and phases from time-domain signals using a linear least-squares procedure. *J Magn Reson 61*:465–474.

Bax A, Ikura M, Kay LE, Torchia DA, Tschudin R. 1989. Comparison of different modes of two-dimensional reverse correlation NMR for the study of proteins. *J Magn Reson 86*:304–310.

Benning MM, Meyer TE, Holden HM. 1994. X-ray structure of the cytochrome c_2 isolated from *Paracoccus denitrificans* refined to 1.7-Å resolution. *Arch Biochem Biophys 310*:460–466.

Braun D, Wider G, Wüthrich K. 1994. Sequence-corrected ^{15}N "random coil" chemical shifts. *J Am Chem Soc 116*:8466–8469.

Chang JP, Morris JG. 1962. Studies on the utilization of nitrate by *Micrococcus denitrificans*. *J Gen Microbiol 29*:301–310.

Clore GM, Szabo A, Bax A, Kay LE, Driscoll PC, Gronenborn AM. 1990. Deviations from the simple two-parameter model-free approach to the interpretation of nitrogen-15 nuclear magnetic relaxation of proteins. *J Am Chem Soc 112*:4989–4991.

Clubb RT, Thanabal V, Wagner G. 1992. Constant-time three-dimensional triple-resonance pulse scheme to correlate intraresidue $^{1}H^{N}$, ^{15}N and $^{13}C'$ chemical shifts in ^{15}N-^{13}C-labelled proteins. *J Magn Reson 97*:213–218.

De Gier JWL, Lubben M, Reijnders WNM, Tipker CA, Slotboom DJ, van Spanning RJM, Stouthamer AH, van der Oost J. 1994. The terminal oxidases of *Paracoccus denitrificans*. *Mol Microbiol 13*:183–196.

Gerhus E, Steinrücke P, Ludwig B. 1990. *Paracoccus denitrificans* cytochrome c_1 gene replacement mutants. *J Bacteriol 172*:2392–2400.

Grzesiek S, Bax A. 1992. Improved 3D triple resonance NMR techniques applied to a 31 kDa protein. *J Magn Reson 96*:432–438.

Kadkhodaei M, Hwang TL, Tang J, Shaka AJ. 1993. A simple windowless mixing sequence to suppress cross relaxation in TOCSY experiments. *J Magn Reson A104*:105–107.

Kay LE, Nicholson LK, Delagio F, Bax A, Torchia DA. 1992. Pulse sequences for removal of the effects of cross correlation between dipolar and chemical shift anisotropy relaxation mechanism on the measurement of heteronuclear T_1 and T_2 values in proteins. *J Magn Reson 97*:359–367.

Kay LE, Torchia DA, Bax A. 1989. Backbone dynamics of proteins as studied by ^{15}N inverse detected heteronuclear NMR spectroscopy: Application to staphylococcal nuclease. *Biochemistry 28*:8972–8979.

Kraulis PJ. 1989. ANSIG: A program for the assignment of protein 1H 2D NMR spectra by interactive graphics. *J Magn Reson 84*:627–633.

Kraulis PJ, Domaille PJ, Campbell-Burk SL, van Aken T, Laue ED. 1994. Solution structure and dynamics of Ras p21.GDP determined by heteronuclear three- and four-dimensional NMR spectroscopy. *Biochemistry 33*:3515–3531.

Lipari G, Szabo A. 1982a. A model free approach to describe molecular motions. I. *J Am Chem Soc 104*:4546–4559.

Lipari G, Szabo A. 1982b. A model free approach to describe molecular motions. II. *J Am Chem Soc 104*:4559–4570.

Lommen A, Ratsma A, Bijlsma N, Canters GW, van Wielink JE, Frank J, Van Beeumen J. 1990. Isolation and characterization of cytochrome c_{550} from the methylamine-oxidizing electron-transport chain of *Thiobacillus versutus*. *Eur J Biochem 192*:653–661.

Majumdar A, Zuiderweg EP. 1993. Improved ^{13}C-resolved HSQC-NOESY spectra in H_2O, using pulsed field gradients. *J Magn Reson A102*:242–245.

Mandel AM, Akke M, Palmer AG. 1995. Backbone dynamics of *Escherichia coli* ribonuclease HI: Correlations with structure and function in an active enzyme. *J Mol Biol 246*:144–163.

Margoliash E, Smith EL, Kreil G, Tuppy H. 1961. Amino acid sequence of horse heart cytochrome *c*. *Nature 192*:1121–1127.

Marion D, Ikura M, Tschudin R, Bax A. 1989. Rapid recording of 2D NMR spectra without phase cycling. Application to the study of hydrogen exchange in proteins. *J Magn Reson 85*:393–397.

Miki K, Sogabe S, Uno A, Ezoe T, Kasai N, Saeda M, Matsuura Y, Miki M. 1994. Application of an automatic molecular-replacement procedure to crystal-structure analysis of cytochrome c_2 from *Rhodopseudomonas viridis*. *Acta Crystallogr D 50*:271–275.

Mitschang L, Cieslar C, Holak TA, Oschkinat H. 1991. Application of the Karhunen-Loewe transformation to the suppression on undesired resonances in three-dimensional NMR. *J Magn Reson 92*:208–217.

Moore GR, Pettigrew GW. 1990. *Cytochromes c. Evolutionary, structural and physiochemical aspects*. Berlin, Germany: Springer-Verlag.

Neidig KP, Geyer M, Görler A, Antz C, Saffrich R, Beneicke W, Kalbitzer HR. 1995. AURELIA, a program for computer-aided analysis of multidimensional NMR spectra. *J Biomol NMR 6*:255–270.

Pascual J, Pfuhl M, Rivas G, Pastore A, Saraste M. 1996. The spectrin repeat folds in a compact three-helix structure in solution. *FEBS Lett 383*:201–207.

Pettigrew GW, Moore GR. 1987. *Cytochromes c. Biological aspects*. Berlin, Germany: Springer-Verlag.

Redfield C, Boyd J, Smith LJ, Smith RA, Dobson CM. 1992. Loop mobility in a four-helix-bundle protein: ^{15}N NMR relaxation measurements on human interleukin-4. *Biochemistry 31*:10431–10437.

Rott MA, Witthuhn VC, Schilke BA, Soranno M, Ali A, Donohue TJ. 1993. Genetic evidence for the role of isocytochrome c_2 in photosynthetic growth of *Rhodobacter sphaeroides* spd mutants. *J Bacteriol 175*:358–366.

Salemme FR, Freer ST, Xuong NgH, Alden RA, Kraut J. 1973. The structure of oxidized cytochrome c_2 of *Rhodospirillum rubrum*. *J Biol Chem 248*:3910–3921.

Samyn B, Berks BC, Page MD, Ferguson SJ, Van Beeumen JJ. 1994. Characterisation and amino acid sequence of cytochrome *c*-550 from *Thiosphaera pantotropha*. *Eur J Biochem 219*:585–594.

Schmid FX, Mayr LM, Mücke M, Schönbrunner ER. 1993. Prolyl isomerases: Role in protein folding. *Adv Protein Chem 44*:25–66.

Shaka AJ, Lee CL, Pines A. 1988. Iterative schemes for bilinear operators; application to spin decoupling. *J Magn Reson 77*:274–293.

Shaka AJ, Parker PB, Freeman R. 1985. Computer-optimized decoupling scheme for wideband applications and low-level operation. *J Magn Reson 64*:547–552.

Sklènar V, Piotto M, Leppik R, Saudek V. 1993. Gradient-tailored water suppression for ^{1}H-^{15}N HSQC experiments optimized to retain full sensitivity. *J Magn Reson 102*:241–245.

Stonehouse J, Shaw GL, Keeler J, Laue ED. 1994. Minimizing sensitivity losses in gradient-selected ^{15}N-^{1}H HSQC spectra of proteins. *J Magn Reson A107*:178–184.

Timkovich R, Dickerson RE. 1976. The structure of *Paracoccus denitrificans* cytochrome c_{550}. *J Biol Chem 251*:4033–4046.

Ubbink M, Campos AP, Teixeira M, Hunt NI, Hill HAO, Canters GW. 1994a. Characterization of mutant Met100Lys of cytochrome *c-550* from *Thiobacillus versutus* with lysine-histidine heme ligation. *Biochemistry 33*:10051–10059.

Ubbink M, Canters GW. 1993. Mutagenesis of the conserved lysine 14 of cytochrome *c*-550 from *Thiobacillus versutus* affects the protein structure and the electron self-exchange rate. *Biochemistry 32*:13893–13901.

Ubbink M, Hunt NI, Hill HAO, Canters GW. 1994b. Kinetics of the reduction of wild type and mutant cytochrome *c*-550 by methylamine dehydrogenase and amicyanin from *Thiobacillus versutus*. *Eur J Biochem 222*:561–571.

Ubbink M, Van Beeumen J, Canters GW. 1992. Cytochrome c_{550} from *Thiobacillus versutus*: Cloning, expression in *Escherichia coli*, and purification of the heterologous holoprotein. *J Bacteriol 174*:3707–3714.

Ubbink M, Warmerdam GCM, Campos AP, Teixeira M, Canters GW. 1994c. The role of lysine 99 of *Thiobacillus versutus* cytochrome *c*-550 in the alkaline transition. *FEBS Lett 351*:100–104.

Van Spanning RJM, De Boer APN, Reijnders WNM, De Gier JWL, De Lorme CO, Stouthamer AH, Westerhoff HV, Harms N, van der Oost J. 1995. Regulation of oxidative-phosphorylation—The flexible respiratory network of *Paracoccus denitrificans*. *J Bioenerg Biomembr 27*:499–512.

Van Spanning RJM, Wansell CW, Harms N, Oltmann LF, Stouthamer AH. 1990. Mutagenesis of the gene encoding cytochrome c_{550} of *Paracoccus denitrificans* and the analysis of the resultant physiological effects. *J Bacteriol 172*:986–996.

Van Spanning RJM, Wansell CW, Reijnders WMN, Harms N, Ras J, Oltmann LF, Stouthamer AH. 1991. A method for introduction of unmarked mutations in the genome of *Paracoccus denitrificans*: Construction of strains with multiple mutations in the genes encoding periplasmic cytochromes c_{550}, c_{551i} and c_{553i}. *J Bacteriol 173*:6962–6970.

Van Wielink JE, Frank Jnz J, Duine JA. 1989. Electron transport from methylamine to oxygen in the Gram-negative bacterium *Thiobacillus versutus*. In: Jongejan JA, Duine JA, eds. *PQQ and Quinoproteins*. Dordrecht, the Netherlands: Kluwer Academic Publishers. pp 269–278.

Wishart DS, Bigam CG, Yao J, Abildgaard F, Dyson HJ, Oldfield E, Markley JL, Sykes BD. 1995. ^{1}H, ^{13}C and ^{15}N chemical shift referencing in biomolecular NMR. *J Biol NMR 6*:135–140.

Wishart DS, Sykes BD. 1994. The ^{13}C chemical-shift index: A simple method for the identification of protein secondary structure using ^{13}C chemical-shift data. *J Biomol NMR 4*:171–180.

Wishart DS, Sykes BD, Richards FM. 1991. Relationship between nuclear magnetic resonance chemical shift and protein secondary structure. *J Mol Biol 222*:311–333.

Wolfram S. 1988. *Mathematica—A system for doing mathematics by computer, v. 2.0*. Champaign, Illinois: Wolfram Research Inc.